Bioorganic & Medicinal Chemistry 19 (2011) 3995–4003

Contents lists available at ScienceDirect

Bioorganic & Medicinal Chemistry

journal homepage: www.elsevier.com/locate/bmc

New microtubule polymerization inhibitors comprising a nitrooxymethylphenyl group

Yasuyuki Kawaratani [a], Tomohiko Harada [a], Yoshiyuki Hirata [a], Yasuo Nagaoka [a], Susumu Tanimura [b], Makio Shibano [c], Masahiko Taniguchi [c], Masahide Yasuda [c], Kimiye Baba [c], Shinichi Uesato [a,*]

[a] Department of Life Science and Biotechnology, Faculty of Chemistry, Materials and Bioengineering, Kansai University, Suita, Osaka 564-8680, Japan
[b] Laboratory of Cell Regulation, Department of Pharmaceutical Sciences, Graduate School of Biomedical Sciences, Nagasaki University, 1-14 Bunkyo-machi, Nagasaki 852-8521, Japan
[c] Osaka University of Pharmaceutical Sciences, 4-20-1 Nasahara, Takatsuki, Osaka 569-1094, Japan

ARTICLE INFO

Article history:
Received 5 April 2011
Revised 16 May 2011
Accepted 16 May 2011
Available online 23 May 2011

Keywords:
Tubulin polymerization inhibitor
Nitrooxymethylphenyl group
M phase regulator
Phospho-histone H3
HCT116 xenograft

ABSTRACT

We have designed cancer antiproliferative compounds, starting from aniline or phenol derivative, which comprise one or two nitrooxymethylphenyl groups as do the hybrid drugs NCX4040 and NCX530. Compound **2a** with *p*-nitrooxymethylbenzoyl-oxy and -amino groups as well as **8a** with a *p*-nitrooxymethylbenzoylamino group showed more promising effects than NCX4040 against human colon and breast cancer cells. Since **2a** and **8a**, but not NCX4040, arrested human colon carcinoma HCT116 cells in the M phase, the former two compounds may inhibit cell growth differently from NCX4040. Merged images of immunofluorescence-stained α-tubulin and Hoechst-stained nuclei in human fibrosarcoma HT1080 cells showed that **2a** and **8a** disrupted microtubule formation just as did vincristine, the tubulin polymerization inhibitor. In experiments in vivo, the intraperitoneal administration of **8a** at 80 mg/kg/day reduced the growth of HCT116 xenografts in nude mice to *T*/*C* 55%.

1. Introduction

NO-donating NSAIDs, developed as hybrid drugs to overcome the gastrointestinal and renal toxicity of traditional NSAIDs, have a protective effect on the gastric mucosa by releasing NO from their nitrooxymethylphenyl group. Two examples are NCX4040 (NO-aspirin)[1–6] and NCX530 (NO-indomethacin)[7–9] (Fig. 1). The former drug has attracted the attention of many medicinal chemists because it showed promising antitumor activity against colon cancers. Later, however, Hulsman et al.[10] proposed that NCX4040 is converted to a quinone methide, which in turn binds to glutathione as an alkylating agent. This causes a reduction in oxidative stress tolerance, leading to the death of cancer cells.

In the present work, we designed aniline or phenol derivatives which comprise a nitrooxymethylphenyl group as do NCX4040 and NCX530, in expectation of diverse activities[1–6,10] derived from its group. Among the new compounds, **2a** and **8a** had a more potent effect than NCX4040 against human colon cancer cells, as well as breast cancer cells. Cell cycle tests revealed that **2a** and **8a**, but not NCX4040, arrested human colon carcinoma HCT116 cells in the G_2/M phase. Therefore, **2a** and **8a** may inhibit cell growth differently from NCX4040. Western blot and flow cytometric analyses showed that these compounds strongly induced phosphorylation of the histone H3 as did vincristine.[11] Thus, we concluded that **2a** and **8a** are a new M phase regulator. Merged images of immunofluorescence-stained α-tubulin and Hoechst-stained nuclei in human fibrosarcoma HT1080 cells showed that **2a** and **8a** disrupted microtubule formation similar to vincristine, a tubulin polymerization inhibitor.[12] In experiments in vivo, the intraperitoneal administration of **8a** at 80 mg/kg/day reduced the growth of HCT116 xenografts in nude mice to *T*/*C* 55%.

2. Chemistry

The bis(nitrooxymethylbenzoyl) derivatives **2a**, **2b**, **4**, and **6** were synthesized as illustrated in Scheme 1. 2-Aminophenol was reacted with *p*- or *m*-(chloromethyl)benzoyl chloride in the presence of pyridine, yielding the *p*-chloromethyl (**1a**) or *m*-chloromethyl derivative (**1b**). These compounds were then treated with $AgNO_3$, giving **2a** and **2b**, respectively. Similarly, compounds **4** and **6** were synthesized via the chloromethyl derivatives **3** and **5**, respectively.

The mononitrooxymethylbenzoyl derivatives **8a**, **8b**, and **13**, as well as **9**, **10**, and **11**, were synthesized as shown in Scheme 2. Aniline was reacted with *p*- or *m*-(chloromethyl)benzoyl chloride to give the *p*-chloromethyl (**7a**) or *m*-chloromethyl derivative (**7b**), respectively. These compounds were treated in the same way as **1a** and **1b**, yielding **8a** and **8b**, respectively. Aniline was also converted into the monobenzoyl derivatives **9** and **10**, respectively.

* Corresponding author. Tel.: +81 6 6368 0834; fax: +81 6 6388 8609.
E-mail address: uesato@ipcku.kansai-u.ac.jp (S. Uesato).

0968-0896/$ - see front matter © 2011 Elsevier Ltd. All rights reserved.
doi:10.1016/j.bmc.2011.05.031

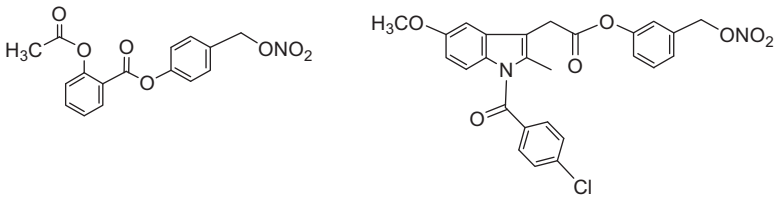

NCX4040 **NCX530**

Figure 1. Structures of NO-donating NSAIDs, NCX4040 and NCX530.

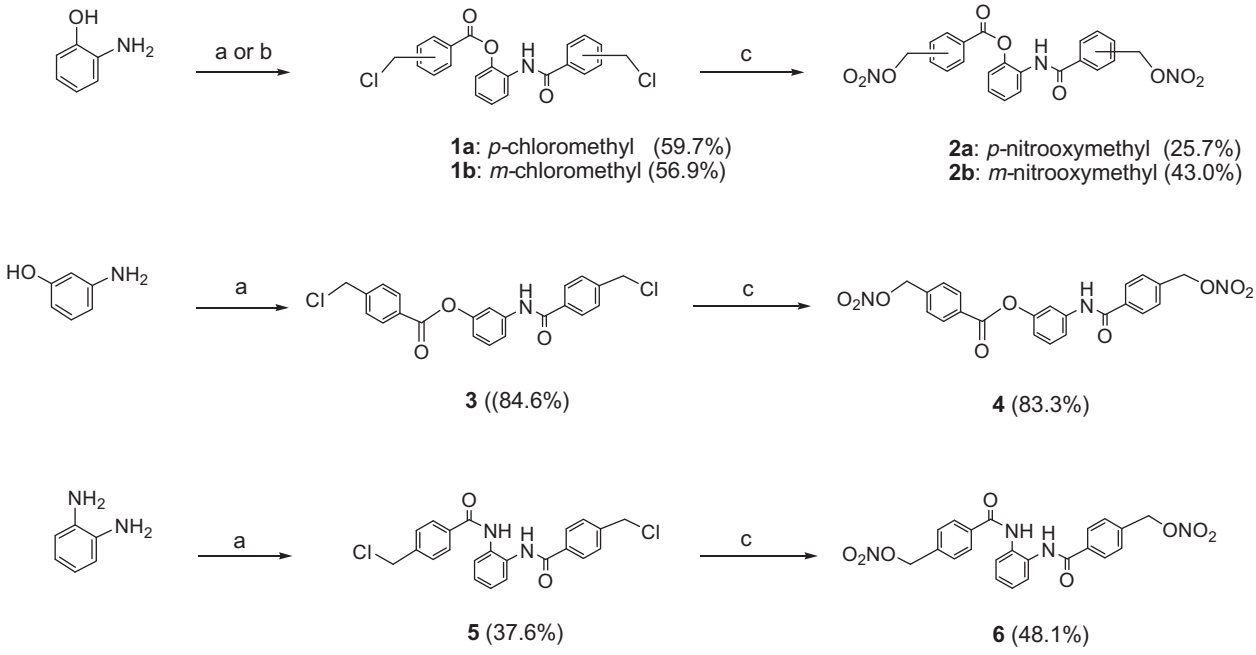

Scheme 1. Reagents and conditions: (a) *p*-(chloromethyl)benzoyl chloride, Py, $CHCl_3$; (b) *m*-(chloromethyl)benzoyl chloride, Py, $CHCl_3$; (c) $AgNO_3$, CH_3CN.

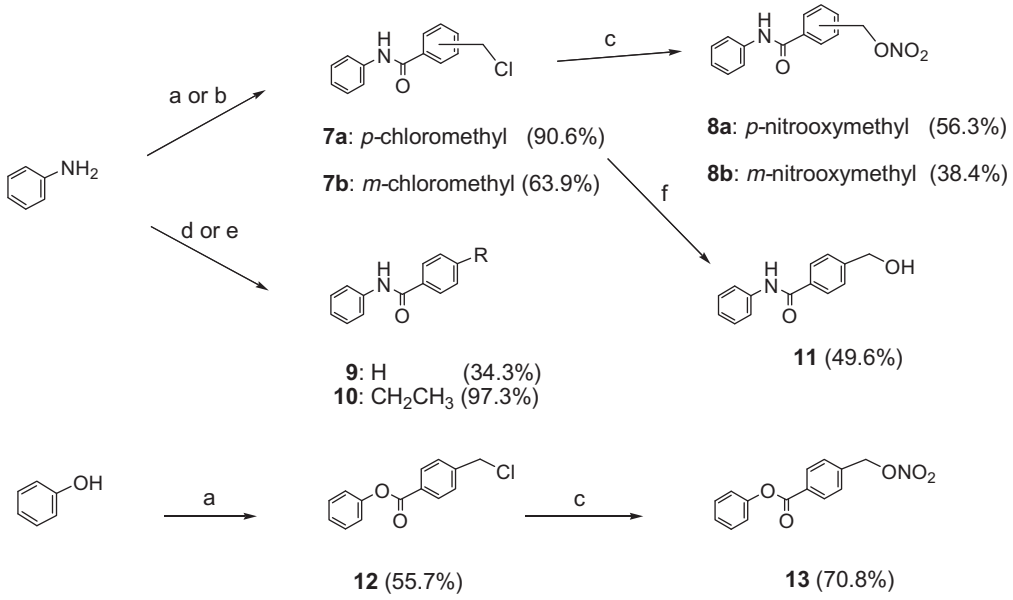

Scheme 2. Reagents and conditions: (a) *p*-(chloromethyl)benzoyl chloride, Py, $CHCl_3$; (b) *m*-(chloromethyl)benzoyl chloride, Py, $CHCl_3$; (c) $AgNO_3$, CH_3CN; (d) benzoyl chloride, Py, $CHCl_3$; (e) *p*-ethylbenzoyl chloride, Py, $CHCl_3$; (f) LiOH, 1,4-dioxane.

Table 1
Inhibitory activities of nitrooxymethylphenyl-possessing compounds and derivatives against the growth of cancer cells

Compound	Colon cancer cells (IC_{50})			Breast cancer cells (IC_{50})		
	HCT116	SW620	SW480	SKBR-3	MCF7	MDA-MB-231
1a	0.6	0.8	6.9	0.6	58.1	0.8
2a	0.7	0.8	3.8	0.7	>100	1.4
2b	47.6	25.8	22.2	18.5	>100	30.0
4	6.2	7.6	8.4	6.3	>100	6.7
6	>100	>100	>100	>100	>100	>100
7a	1.2	0.8	0.9	0.7	54.3	0.8
8a	0.6	0.8	0.8	0.7	>100	0.8
8b	19.3	8.4	13.3	8.2	>100	8.4
9	>100	>100	>100	>100	>100	>100
10	>100	>100	>100	>100	>100	>100
11	24.8	>100	>100	9.8	>100	>100
13	17.9	16.9	80.7	50.1	>100	47.7
NCX4040	68.0	15.1	19.1	30.5	>100	14.4

Furthermore, **7a** was hydrolyzed with LiOH to afford the alcohol **11**. Phenol was converted, via the chloromethyl derivative **12**, into **13** in the conventional manner.

3. Results and discussion

3.1. Antiproliferative activities and structure–activity relationships of the nitrooxymethylbenzoyl derivatives and related compounds

Compound **2a**, comprising *p*-nitrooxymethylbenzoyl-oxy and -amino groups, inhibited significantly the growth of the human colon (IC_{50}: 0.7–3.8 μM) and breast (IC_{50}: 0.7–1.4 μM) cancer cells except for human breast MCF7 cells as shown in Table 1. However, **6**, possessing two *p*-nitrooxymethylbenzoylamino groups, as well as **2b**, having *m*-nitrooxymethylbenzoyl-oxy and -amino groups, had greater IC_{50} values than **2a**. Interestingly, **8a**, with a *p*-nitrooxymethylbenzoylamino group, inhibited the growth of these cancer cells to nearly the same extent (IC_{50}: 0.6–0.8 μM for the colon cancer cells; 0.7–0.8 μM for the breast cancer cells) as **2a**. In contrast, **13**, with a *p*-nitrooxymethylbenzoyloxy group, exhibited only weak effects. Furthermore, the synthetic intermediates comprising a chloromethylbenzoylamino group, **1a** and **7a**, showed comparatively strong activities, whereas **9**, **10** and **11**, not having a leaving group such as Cl and ONO_2, had little or no effect. The IC_{50} values of **2a** and **8a** for the growth of normal human fibroblast CCD-1059SK cells could not be determined even at 200 μM.

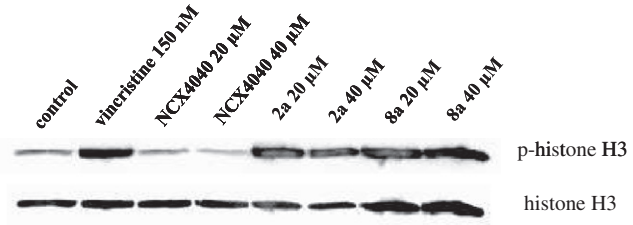

Figure 3. Mitotic checkpoint analysis by Western blotting. HCT116 cells were treated with **2a**, **8a**, NCX4040, or vincristine for 24 h. Cells were lysed to extract crude histone proteins. The Western blot analysis was performed with crude histone samples using an antibody specific to phospho-histone H3 (Ser-10), or total histone H3. Results are representative of five independent experiments.

These findings suggest that the framework of **8a** and the para orientation of its nitrooxymethyl group on the benzene ring as well as an electronegative substituent such as ONO_2 and Cl are essential to the antiproliferative activities. Additional introduction of a nitrooxymethylbenzoyl-oxy (**2a**, **2b** and **4**) or -amino (**6**) group seems to be unnecessary. The impotency of **13** could be explained by a higher rotatability of its *p*-nitrooxymethylbenzoyloxy chain on a benzene ring than that of the *p*-nitrooxymethylbenzoylamino chain in **8a**; this might diminish the interaction between **13** and an active site.

3.2. Effect of 2a and 8a on the cell cycle

Both **2a** and **8a** regulated HCT116 cells in the G_2/M phase of the cell cycle at 20 μM in 24 h as did vincristine, and the percentage

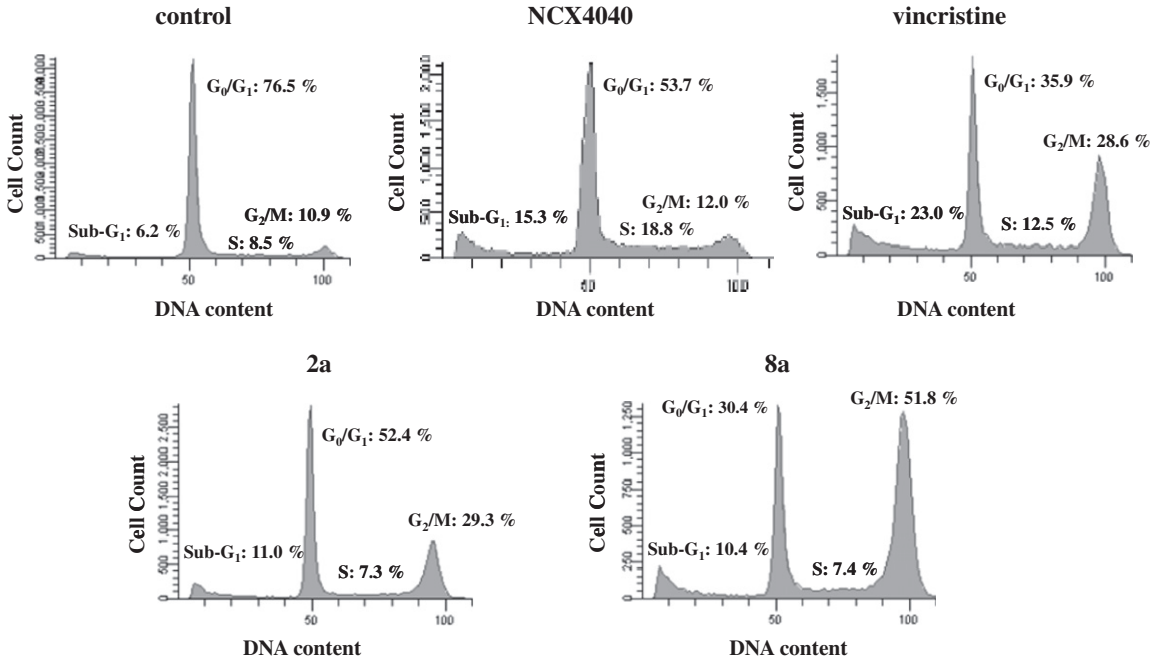

Figure 2. Effects of **2a** and **8a** on the cell cycle in HCT116 cells. Cells were treated with a BD Cycletest™ Plus DNA reagent Kit. Data shown are those for treatment for 24 h with **2a**, **8a** (each at 20 μM), NCX4040 (at 40 μM), or vincristine (at 150 nM) or for the control (no treatment) for 24 h. They are representative of five independent experiments.

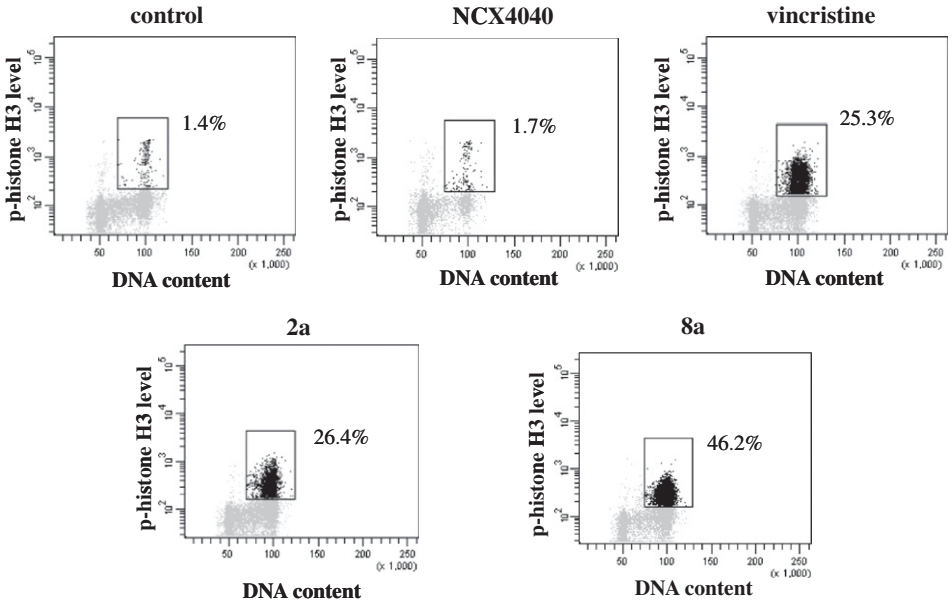

Figure 4. Mitotic checkpoint analysis by flow cytometry. HCT116 cells were treated with **2a**, **8a** (each at 20 μM), NCX4040 (at 40 μM), or vincristine (at 150 nM) for 24 h. Cells in mitosis were determined by staining with propidium iodide and phospho-histone H3 (Ser-10) antibody followed by FITC-conjugated secondary antibody. The percentage of cells with tetraploid DNA and a high level of phospho-histone H3 was determined by FACS. Numbers in the upper right corners indicate percentages of mitotic cells in each sample. They are representative of three independent experiments.

ratio (170.4%) of the G_2/M phase to G_0/G_1 phase cells on the incubation with **8a** was much higher than the ratio (55.9%) on the incubation with **2a** (Fig. 2). However, NCX4040 did not arrest the cells in the G_2/M phase even at 40 μM. These compounds induced apoptosis as suggested by the appearance of a sub G_1 population in the DNA histograms. These results suggested that **2a** and **8a** exhibited inhibitory activities different from NCX4040.

To determine whether these two compounds arrest HCT116 cells in the G_2 or M phase, the phosphorylation of histone H3 at Ser 10 was analyzed by Western blotting (Fig. 3) as well as by flow cytometry (Fig. 4) using an anti-phospho-histone H3 (Ser 10) antibody. Histone H3 phosphorylated at Ser10 is a well-established mitotic marker.[13–16] In the Western blot assay, the expression of the phospho-histone H3 was enhanced by **2a** and **8a** as in the case of vincristine, but not by NCX4040. Furthermore, in the flow cytometric analysis, the proportion of phospho-histone H3 positive cells was increased from 1.4% to 26.4% by **2a** and 46.2% by **8a** (at 20 μM in 24 h), but not increased by NCX4040 (1.7% at 40 μM in 24 h). The findings indicated that HCT116 cells accumulated in the M phase on the incubation with **2a** or **8a** and the M phase population was much larger in the cells given **8a** than in those given **2a**.

3.3. Determination of apoptosis induced by 2a and 8a

The appearance of a sub G_1 population among the HCT116 cells treated with **2a** and **8a** (Fig. 2) suggested apoptosis, which was confirmed by a TUNEL assay. As shown in Fig. 5, the percentage of TUNEL-positive cells was 36.4% for **2a** and 24.2% for **8a** at 20 μM

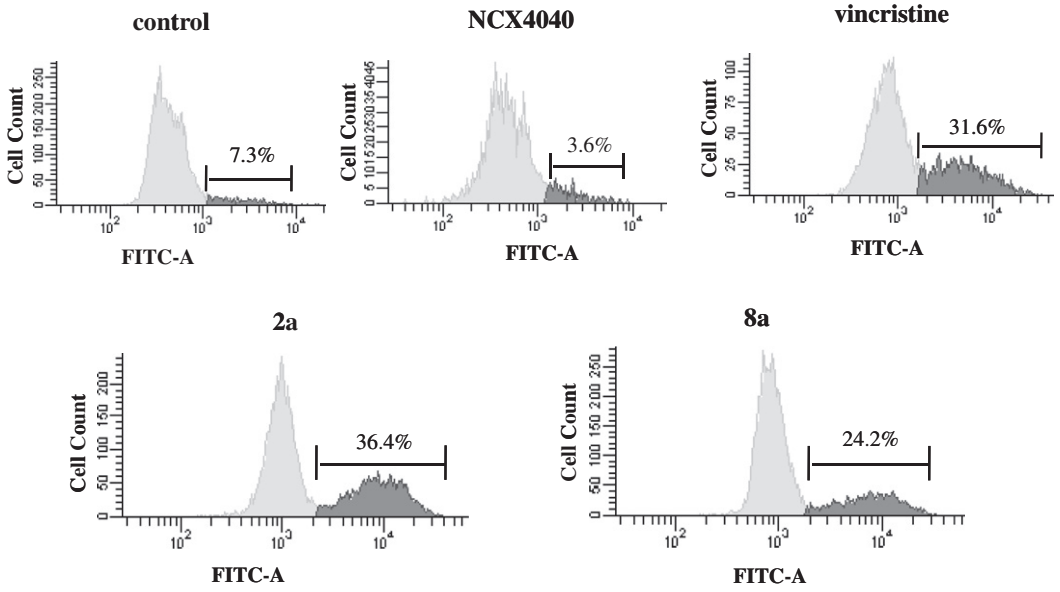

Figure 5. FITC–TUNEL staining cell analysis by flow cytometry. HCT116 cells were incubated with **2a**, **8a** (each at 20 μM), NCX4040 (at 40 μM), or vincristine (at 150 nM) for 48 h and then treated as indicated in Materials and methods. Percentages of FITC–TUNEL-positive cells are indicated. Values are representative of five independent experiments.

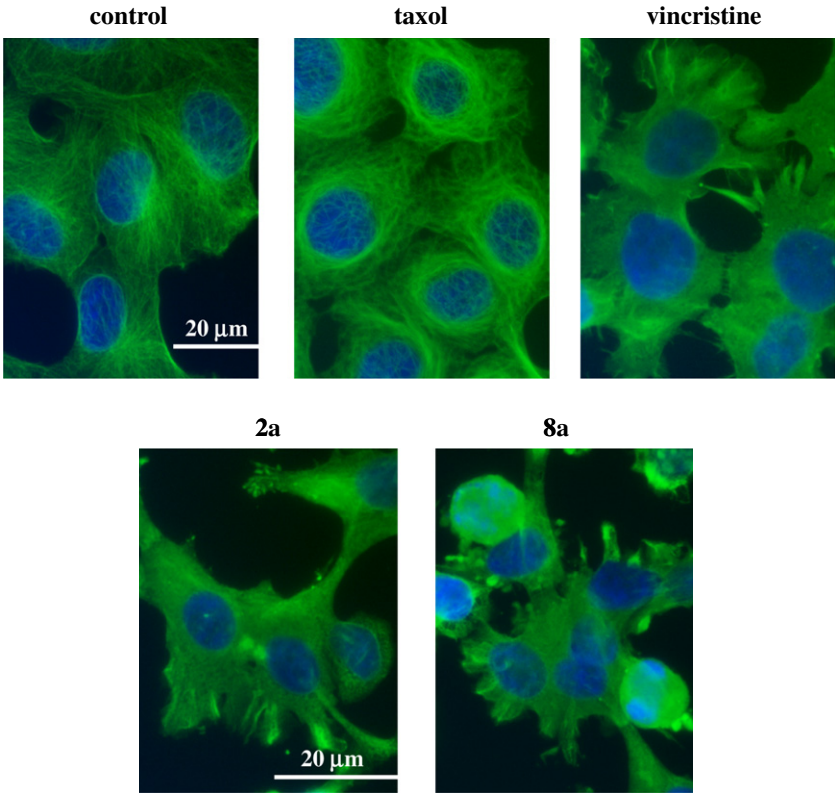

Figure 6. Examination of the ability of **2a** and **8a** to affect the microtubule structures. HT1080 cells were cultured with **2a** (10 μM), **8a** (10 μM), taxol (100 nM), or vincristine (100 nM) for 4 h and then treated as reported previously.[17] Cells were imaged using a fluorescence microscope.

in 48 h, whereas it was 3.6% for NCX4040 at 40 μM. The values were 4–5% for all these compounds at 24 h (data not shown). These results, as well as the effects on the cell cycle, suggested that **8a** might have a more cytostatic effect on HCT116 cells than **2a** though these compounds suppressed cell growth to the same extent.

3.4. Effect of 2a and 8a on microtubule organization

The effects of **2a**, **8a**, vincristine and taxol on the microtubule structures were compared in HT1080 human fibrosarcoma cells to distinguish whether the former two compounds inhibited the polymerization of tubulin (to destabilize microtubule structures) or the de-polymerization of tubulin (to stabilize microtubule structures).[17] Fig. 6 illustrates merged images of immunofluorescence-stained α-tubulin (green) and Hoechst-stained nuclei (blue) in HT1080 cells. It was indicated that both **2a** and **8a**, like vincristine, but unlike taxol,[18] disrupted microtubule formation. In the next experiment, we thus tried to examine how **2a** and **8a** inhibited microtubule development. A tubulin polymerization assay was conducted using porcine brain tubulin by measuring the intensity of fluorescence emission at 460 nm of microtubule-bound DAPI.[19] As shown in Figure 7, **2a** and **8a**, though not strongly, reduced a polymer mass, respectively. This result suggested that the interaction of **2a** or **8a** with tubulin might be, at least in part, responsible for the disruption of tubulin-polymerization. We assumed that **2a** and **8a** bound to tubulin as alkylating agents after or with the removal of -ONO_2. It seems however necessary to examine the in vivo behavior of these compounds in understanding their mode of action in more detail.

3.5. In vivo evaluation of 8a

Compound **8a**, having comparatively low IC_{50} values as well as a cytostatic effect on the HCT116 cells, could be applied as a cancer

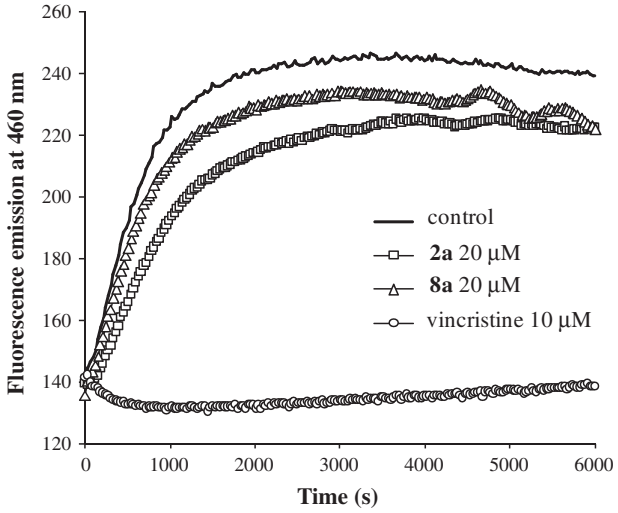

Figure 7. Effects of **2a** and **8a** on tubulin assembly. Tubulin (2.0 mg/mL) was dissolved in General Tubulin Buffer. The reaction was performed with **2a**, **8a**, vincristine or no reagent (control). The mixture was incubated at 37 °C. Polymerization was measured over 100 min by reading the increase in fluorescent emission at 460 nm in the kinetic mode with excitation at 340 nm. Values are representative of four independent experiments.

therapeutic agent with few side effects. We thus conducted antitumor tests of **8a** using xenografts of HCT116 cells in nude mice. The compound was administered intraperitoneally at a dose of 50 or 80 mg/kg/day over 16 days according to the schedules indicated in Figure 8A. Compound **8a** suppressed the growth of the xenografts to *T*/*C*: 55% in 21 days. Weight loss was similar between the **8a**-treated and control groups and was not significant throughout the treatment period (Fig. 8B).

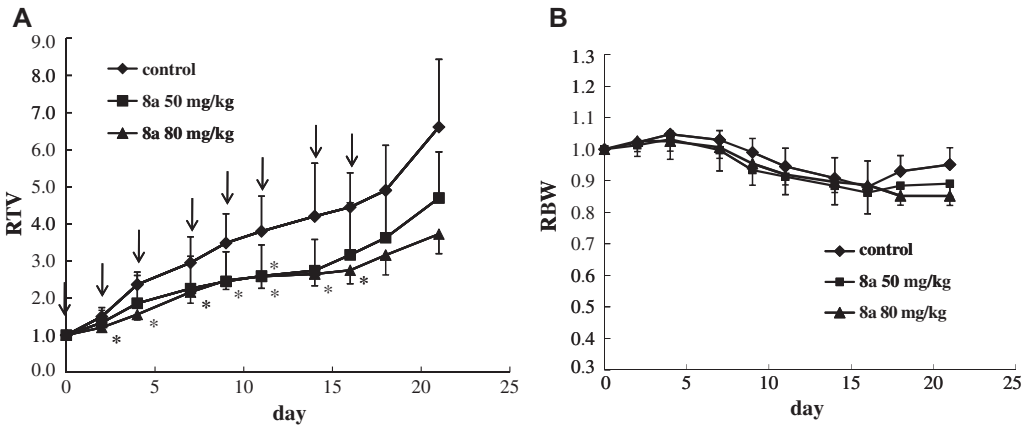

Figure 8. Effects of **8a** on HCT116 cell-inoculated xenografts in vivo. The effects of **8a** (■ 50 mg/kg; ▲ 80 mg/kg) on tumor volume (**8A**) as well as relative body weight changes (**8B**) were examined as described in Materials and methods. The relative tumor volume (RTV) was calculated by dividing the tumor volume at each day by the tumor volume at day 0. The relative body weight (RBW) was calculated as the ratio of body weight at each day to that at day 0. (♦) represents the control group. Compounds were intraperitoneally administered to mice at days 0, 2, 4, 7, 9, 11, 14 and 16. Vertical bars indicate standard errors. The asterisks denote significant difference (p <0.01 by two-tailed Student t-test) for tumor volume with **8a** versus the control.

4. Conclusion

Compounds **2a** and **8a**, each possessing a *p*-nitrooxymethylphenyl group, showed stronger antiproliferative activities than NCX4040 against the human cancer cell lines. Both compounds arrested HCT116 cells in the M phase of the cell cycle and inhibited microtubule formation. The intraperitoneal administration of **8a** reduced the growth of human HCT116 cancer xenografts in nude mice to *T*/*C* 55%. Thus, **8a** warrants further tests with other human cancer xenografts to identify its effectiveness as an antitumor agent.

5. Experimental

5.1. General

Melting points were determined on a Yanaco MP-500D micro-melting point apparatus and are uncorrected. IR spectra in KBr were recorded on a Shimadzu FTIR-8400 infrared spectrophotometer. Low-resolution (LR)-FAB-MS spectra were measured on a JEOL JMS-HX 100, whereas high-resolution (HR)- and LR-FAB-MS spectra, on a JEOL Tandem MStation JMS-700. ^{1}H NMR spectra were recorded on a JEOL EX-400 (400 MHz), unless otherwise stated, in $CDCl_3$ with tetramethylsilane as an internal standard. Analytical TLC and PLC were performed using Silica gel 60 F254 (Merck, 0.25 and 1 mm, respectively) glass plates. Column chromatography was performed using Silica Gel 60 (70–230 mesh ASTM). All the solvents were dried over Na_2SO_4, and evaporated in vacuo. The HCT116, SW480, SW620 (human colon carcinoma), SKBR-3, MCF7, MDA-MB-231 (human breast carcinoma) and CCD-1059SK (human normal fibroblast) cell lines were purchased from American Tissue Culture Collection. The Cell Counting Kit for the WST-1 assay was obtained from DOJINDO.[20] NCX4040 was prepared as reported prior.[10] BD Cycletest™ Plus DNA reagent Kit was purchased from Becton Dickinson and Company. The TUNEL assay reagent, DeadEnd™ Fluorometric TUNEL System, was obtained from Promega. Results of flow cytometry were collected with a FACSCant II flow cytometer (Becton Dickinson and Company). The tubulin polymerization assay was conducted according to the catalogue (Tubulin Polymerization Assay, Cat. #BK011P) of Cytoskeleton, using General Tubulin Buffer (Cat. #BST01-001), Tubulin Glycerol Buffer (Cat. #BST05-001), GTP (Cat. #BST06-001), Tubulin (porcine brain) (Cat. #T240-A) (Cytoskeleton) and DAPI solution (DOJINDO). Female BALB/c-nu.nu nude mice (5 weeks of age) were purchased from Japan SLC Inc. Animals were housed and experiments were performed according to guidelines stipulated by the Osaka University of Pharmaceutical Sciences Animal Care and Use Committee.

5.2. Chemistry

5.2.1. 2-(4-(Chloromethyl)benzamido)phenyl 4-(chloromethyl) benzoate (1a)

To a solution of *o*-aminophenol (0.33 g, 3.00 mmol) in $CHCl_3$ (5 mL) were added pyridine (0.97 mL, 12.00 mmol) and *p*-(chloromethyl)benzoyl chloride (1.13 g, 6.00 mmol), and the mixture was stirred at 0 °C for 2 h. The mixture was successively diluted with $CHCl_3$, washed with 1% HCl and satd. $NaHCO_3$ and brine, dried, and concentrated. The resulting solid was recrystallized from $CHCl_3$ and *n*-hexane to give **1a** (0.74 g, 1.79 mmol, 59.7%) as colorless needles. Mp 151.0–152.5 °C. IR: 1722.3, 1672.2, 1454.2, 1253.6, 1178.4, 750.3 cm^{-1}. ^{1}H NMR: δ 5.50 (2H, s), 5.53 (2H, s), 7.03–7.06 (1H, m), 7.43–7.44 (2H, m), 7.54 (2H, d, J = 8.0 Hz), 7.56 (2H, s), 7.75 (1H, t, J = 1.4 Hz), 7.86 (1H, s), 7.90 (2H, d, J = 8.0 Hz), 8.24 (2H, d, J = 8.4 Hz). FAB-MS m/z: 414 (M+H) $^+$. HR-FAB-MS m/z: (M+H)$^+$calcd for $C_{22}H_{18}Cl_2NO_3$, 414.0662; found, 414.0670.

5.2.2. 2-(4-(Nitrooxymethyl)benzamido)phenyl 4-(nitrooxymethyl)benzoate (2a)

A suspension of $AgNO_3$ (0.41 g, 2.40 mmol) in CH_3CN (2 mL) was added to a solution of **1a** (0.21 g, 0.50 mmol) in CH_3CN (5 mL), and the mixture was stirred at 60 °C for 4 h under light-shielding. The mixture was filtered off through Celite to separate insoluble materials, and the filtrate was concentrated. The resulting solid was purified on silica gel column with EtOAc: $CHCl_3$: *n*-hexane (2:1:1) as an eluent and recrystallized from EtOAc and *n*-hexane, affording **2a** (0.06 g, 0.13 mmol, 25.7%) as colorless needles. Mp 136.2 °C. IR: 3346.3, 1720.4, 1674.1, 1537.2, 1259.4, 887.2, 750.3 cm^{-1}. ^{1}H NMR: δ 4.92 (2H, s), 5.10 (2H, s), 7.36 (4H, m), 7.43 (2H, d, J = 8.8 Hz), 7.57 (2H, d, J = 8.4 Hz), 7.77 (2H, d, J = 5.2 Hz), 7.97 (1H, br s), 8.25 (2H, d, J = 4.4 Hz). FAB-MS m/z: 468 (M+H)$^+$. HR-FAB-MS m/z: (M+H)$^+$ calcd for $C_{22}H_{18}N_3O_9$, 468.1044; found, 468.1046.

5.2.3. 2-(3-(Chloromethyl)benzamido)phenyl 3-(chloromethyl) benzoate (1b)

Compound **1b** was synthesized using *o*-aminophenol (0.11 g, 1.00 mmol), pyridine (0.50 mL, 6.21 mmol), and *m*-(chloromethyl)benzoyl chloride (0.34 mL, 2.40 mmol) in the same way as **1a** (colorless needles, 0.24 g, 0.57 mmol, 56.9%). Mp 154.7–157.3 °C. IR: 2399.3, 1215.1, 754.1 cm^{-1}. ^1H NMR: δ 4.52 (2H, s), 4.66 (2H, s), 7.37–7.41 (3H, m), 7.49–7.56 (2H, m), 7.72 (2H, d, J = 8.0 Hz), 7.77 (1H, s), 8.04 (1H, br s), 8.20 (2H, d, J = 7.6 Hz), 8.26 (1H, s), 8.32 (1H, d, J = 7.6 Hz). FAB-MS m/z: 414 $(M+H)^+$. HR-FAB-MS m/z: $(M+H)^+$ calcd for $C_{22}H_{18}Cl_2NO_3$, 414.0662; found, 414.0669.

5.2.4. 2-(3-(Nitrooxymethyl)benzamido)phenyl 3-(nitrooxymeth yl)benzoate (2b)

Compound **2b** was synthesized using $AgNO_3$ (3.92 g, 23.0 mmol) and **1b** (0.87 g, 2.11 mmol) in the same way as **2a** (colorless needles, 0.42 g, 0.90 mmol, 43.0%). Mp 119.6–123.6 °C. IR: 3018.4, 2399.3, 1215.1, 754.1, 669.3, cm^{-1}. ^1H NMR: δ 5.38 (2H, s), 5.50 (2H, s), 7.30–7.33 (2H, m), 7.37 (1H, t, J = 6.8 Hz), 7.46 (1H, t, J = 7.6 Hz), 7.54 (1H, d, J = 7.2 Hz), 7.60 (1H, t, J = 7.6 Hz), 7.72 (1H, d, J = 7.6 Hz), 7.78 (2H, d, J = 6.0 Hz), 8.00 (1H, br s), 8.27 (3H, d, J = 4.8 Hz). FAB-MS m/z: 468 $(M+H)^+$. HR-FAB-MS m/z: $(M+H)^+$ calcd for $C_{22}H_{18}N_3O_9$, 468.1044; found, 468.1052.

5.2.5. 3-(4-(Chloromethyl)benzamido)phenyl 4-(chloromethyl) benzoate (3)

Compound **3** was synthesized using *m*-aminophenol (0.50 g, 4.58 mmol), pyridine (0.88 mL, 11.00 mmol), and *p*-(chloromethyl)benzoyl chloride (2.08 g, 11.00 mmol) in the same way as **1a** (colorless needles, 1.60 g, 3.87 mmol, 84.6%). Mp 130.0–131.9 °C. IR: 1737.7, 1267.1, 1253.6, 1215.1, 1151.4 cm^{-1}. ^1H NMR: δ 4.64 (2H, s), 4.66 (2H, s), 7.02–7.05 (1H, m), 7.45–7.47 (2H, m), 7.52–7.56 (4H, m), 7.73 (1H, t, J = 6.0 Hz), 7.89 (2H, d, J = 2.0 Hz), 7.88 (1H, s), 8.20 (2H, d, J = 4.4 Hz). FAB-MS m/z: 414 $(M+H)^+$. HR-FAB-MS m/z: $(M+H)^+$ calcd for $C_{22}H_{18}Cl_2NO_3$, 414.0662; found, 414.0677.

5.2.6. 3-(4-(Nitrooxymethyl)benzamido)phenyl 4-(nitrooxymeth yl)benzoate (4)

Compound **4** was synthesized using $AgNO_3$ (0.77 g, 9.68 mmol) and **3** (1.00 g, 2.42 mmol) in the same way as **2a** (colorless needles, 0.94 g, 2.02 mmol, 83.3%). Mp 130.4–133.1 °C. IR: 1643.2, 1280.6, 1213.1, 850.5, 779.2 cm^{-1}. ^1H NMR: δ 5.50 (2H, s), 5.53 (2H, s), 7.03–7.06 (1H, m), 7.41–7.46 (2H, m), 7.53–7.56 (4H, m), 7.75 (1H, s), 7.86 (1H, s), 7.90 (2H, d, J = 8.0 Hz), 8.24 (2H, d, J = 8.0 Hz). FAB-MS m/z: 468 $(M+H)^+$. HR-FAB-MS m/z: $(M+H)^+$ calcd for $C_{22}H_{18}N_3O_9$, 468.1044; found, 468.1055.

5.2.7. *N*,*N*′-(1,2-Phenylene)bis(4-(chloromethyl)benzamide) (5)

Compound **5** was synthesized using *o*-phenylene diamine (0.22 g, 2.00 mmol), pyridine (0.39 mL, 4.80 mmol), and *p*-(chloromethyl)benzoyl chloride (0.91 g, 4.80 mmol) in the usual way (colorless needles, 0.94 g, 0.75 mmol, 37.6%). Mp 189.9–191.4 °C. IR: 1643.2, 1504.4, 1305.7, 1272.9, 754.1, 707.8, 675.0 cm^{-1}. ^1H NMR: δ 4,65 (4H, s), 6.95–7.00 (2H, m), 7.41–7.43 (2H, m), 7.53 (4H, d, J = 8.4 Hz), 7.98 (4H, d, J = 8.4 Hz), 9.25 (2H, s). FAB-MS m/z: 413 $(M+H)^+$. HR-FAB-MS m/z: $(M+H)^+$ calcd for $C_{22}H_{19}Cl_2N_2O_2$, 413.0824; found, 413.0821.

5.2.8. (4,4′-(1,2-Phenylenebis(azanediyl))bis(oxomethylene)bis (4,1-phenylene))bis(methylene) dinitrate (6)

Compound **6** was synthesized using $AgNO_3$ (0.68 g, 4.00 mmol) and **5** (0.41 g, 1.00 mmol) in the conventional manner (colorless needles, 0.22 g, 0.48 mmol, 48.1%). Mp 152.5–158.2 °C. IR: 1629.7, 1280.6, 856.3, 754.1 cm^{-1}. ^1H NMR: δ 5.50 (4H, s), 7.05–7.07 (2H, m), 7.45–7.47 (2H, m), 7.54 (4H, d, J = 7.6 Hz), 8.01 (4H, d, J = 8.0 Hz), 9.19 (2H, s). FAB-MS m/z: 467 $(M+H)^+$. HR-FAB-MS m/z: $(M+H)^+$ calcd for $C_{22}H_{19}N_4O_8$, 467.1204; found, 467.1205.

5.2.9. 4-(Chloromethyl)-*N*-phenylbenzamide (7a)

Compound **7a** was synthesized using aniline (0.27 mL, 3.00 mmol), pyridine (0.29 mL, 3.60 mmol), and *p*-chloromethylbenzoyl chloride (0.68 g, 3.60 mmol) in the conventional manner (colorless needles, 0.67 g, 2.72 mmol, 90.6%). Mp 164.5–166.3 °C. IR: 3346.3, 1654.8, 1598.9, 1529.4, 1438.8, 1325.0 cm^{-1}. ^1H NMR: δ 4.64 (2H, s), 7.17 (1H, t, J = 8.0 Hz), 7.39 (2H, t, J = 8.0 Hz), 7.52 (2H, d, J = 8.0 Hz), 7.63 (2H, d, J = 8.0 Hz), 7.78 (1H, br s), 7.87 (2H, d, J = 8.0 Hz). FAB-MS m/z: 246 $(M+H)^+$. HR-FAB-MS m/z: $(M+H)^+$ calcd for $C_{14}H_{13}ClNO$, 246.0686; found, 246.0684.

5.2.10. 4-(Phenylcarbamoyl)benzyl nitrate (8a)

Compound **8a** was synthesized using $AgNO_3$ (1.70 g, 5.00 mmol) and **7a** (0.54 g, 1.97 mmol) in the conventional manner (colorless needles, 0.30 g, 1.11 mmol, 56.3%). Mp 168.0–170.9 °C. IR: 3018.4, 2399.3, 1215.1, 786.9, 754.1, 669.3 cm^{-1}. ^1H NMR: δ 5.50 (2H, s), 7.18 (1H, t, J = 6.8 Hz), 7.39 (2H, t, J = 8.0 Hz), 7.53 (2H, d, J =7.6 Hz), 7.63 (2H, d, J = 8.0 Hz), 7.80 (1H, br s), 7.91 (2H, d, J = 8.0 Hz). FAB-MS m/z: 273 $(M+H)^+$. HR-FAB-MS m/z: $(M+H)^+$ calcd for $C_{14}H_{13}N_2O_4$, 273.0876; found, 273.0876.

5.2.11. 3-(Chloromethyl)-*N*-phenylbenzamide (7b)

Compound **7b** was synthesized using aniline (0.46 mL, 5.00 mmol), pyridine (0.48 mL, 6.00 mmol), and *m*-(chloromethyl)benzoyl chloride (0.85 mL, 6.00 mmol) in the conventional manner (colorless needles, 0.78 g, 3.20 mmol, 63.9%). Mp 127.7–129.2 °C. IR: 3018.4, 1222.8, 1207.4, 790.8, 727.1, 667.3 cm^{-1}. ^1H NMR: δ 4,66 (2H, s), 7.18 (1H, t, J = 8.0 Hz), 7.38 (2H, t, J = 7.6 Hz), 7.50 (1H, t, J = 7.6 Hz), 7.59 (1H, d, J = 7.6 Hz), 7.65 (2H, d, J = 7.6 Hz), 7.82 (1H, d, J = 7.6 Hz), 7.90 (1H, s). FAB-MS m/z: 246 $(M+H)^+$. HR-FAB-MS m/z: $(M+H)^+$ calcd for $C_{14}H_{13}ClNO$, 246.0686; found, 246.0690.

5.2.12. 3-(Phenylcarbamoyl)benzyl nitrate (8b)

Compound **8b** was synthesized using $AgNO_3$ (1.36 g, 8.00 mmol) and **7b** (0.50 g, 2.04 mmol) in the conventional manner (colorless needles, 0.21 g, 0.78 mmol, 38.4%). Mp 94.1–95.3 °C. IR: 3018.4, 1209.3, 785.0, 731.0, 669.3 cm^{-1}. ^1H NMR: δ 5.51 (2H, s), 7.18 (1H, t, J = 7.2 Hz), 7.39 (2H, t, J = 7.6 Hz), 7.54 (1H, t, J = 7.6 Hz), 7.60 (1H, d, J = 7.2 Hz), 7.64 (2H, d, J = 8.0 Hz), 7.79 (1H, br s), 7.89 (1H, d, J = 7.6 Hz), 7.92 (1H, s). FAB-MS m/z: 273 $(M+H)^+$. HR-FAB-MS m/z: $(M+H)^+$ calcd for $C_{14}H_{13}N_2O_4$, 273.0876; found, 273.0875.

5.2.13. *N*-Phenylbenzamide (9)

Compound **9** was synthesized using aniline (0.09 mL, 1.00 mmol), pyridine (0.08 mL, 1.00 mmol), and benzoyl chloride (0.14 mL, 1.20 mmol) in the conventional manner (colorless needles, 0.68 g, 0.34 mmol, 34.3%). Mp 158.4–162.2 °C. IR: 3301.9, 1656.7, 1535.2, 1438.8, 750.3 cm^{-1}. ^1H NMR: δ 7.16 (1H, t, J = 7.6 Hz), 7.38 (2H, t, J = 7.6 Hz), 7.48–7.58 (3H, m), 7.65 (2H, d, J = 7.6 Hz), 7.82 (1H, br s), 7.88 (2H, d, J = 7.2 Hz). FAB-MS m/z: 198 $(M+H)^+$. HR-FAB-MS m/z: $(M+H)^+$ calcd for $C_{13}H_{12}NO$, 198.0920; found, 198.0923.

5.2.14. 4-Ethyl-*N*-phenyl benzamide (10)

Compound **10** was synthesized using aniline (0.09 mL, 1.00 mmol), pyridine (0.08 mL, 1.00 mmol), and *p*-ethylbenzoyl chloride (0.18 mL, 1.20 mmol) in the conventional manner (colorless needles, 0.22 g, 0.97 mmol, 97.3%). Mp 119.9–123.4 °C. IR:

3300.0, 1649.0, 754.1, 518.8 cm^{-1}. ^1H NMR: δ 1.28 (3H, t, J = 8.0 Hz), 2.73 (2H, q, J = 8.0 Hz), 7.14 (1H, t, J = 7.2 Hz), 7.31 (2H, d, J = 8.0 Hz), 7.36 (2H, t, J = 7.6 Hz), 7.64 (2H, d, J = 8.0 Hz), 7.79 (2H, d, J = 8.0 Hz). FAB-MS m/z: 226 $(M+H)^+$. HR-FAB-MS m/z: $(M+H)^+$ calcd for $C_{15}H_{16}NO$, 226.1233; found, 226.1233.

5.2.15. 4-(Hydroxymethyl)-*N*-phenyl benzamide (11)

To a solution of **7a** (0.10 g, 0.41 mmol) in 1,4-dioxane (5 mL) was added aq LiOH (5 mL, 5.00 mmol), and the mixture was stirred at room temperature for 72 h. The reaction mixture was successively diluted with $CHCl_3$, washed with satd. $NaHCO_3$ and brine, dried, and concentrated. The resulting solid was purified on silica gel column with EtOAc/toluene (1:1) as an eluent and recrystallized from $CHCl_3$ and *n*-hexane, affording **11** (0.05 g, 0.20 mmol, 49.6%) as colorless needles. Mp 143.2–146.3 °C. IR: 3290.3, 2945.1, 2833.2, 2356.9, 2337.6, 1028.0 cm^{-1}. ^1H NMR (DMSO-d6): δ 4.80 (2H, s), 7.16 (1H, t, J = 6.3 Hz), 7.38 (2H, t, J = 7.8 Hz), 7.50 (2H, d, J = 7.8 Hz), 7.65 (2H, d, J = 8.3 Hz), 7.79 (1H, br s), 7.88 (2H, d, J = 7.8 Hz). ESI-MS m/z: 228.2 $(M+H)^+$. HR-FAB-MS m/z: $(M+H)^+$ calcd for $C_{14}H_{14}NO_2$, 228.1025; found, 228.1023.

5.2.16. Phenyl 4-(chloromethyl)benzoate (12)

Compound **12** was synthesized using phenol (0.09 g, 1.00 mmol), pyridine (0.10 mL, 1.20 mmol), and *p*-(chloromethyl)benzoyl chloride (0.23 g, 1.20 mmol) in the conventional manner (colorless needles, 0.14 g, 0.56 mmol, 55.7%). Mp 72.2–76.6 °C. IR: 1730.0, 1274.9, 1195.8, 1072.3, 742.5 cm^{-1}. ^1H NMR: δ 4.63 (2H, s), 7.21 (2H, d, J = 8.4 Hz), 7.27 (1H, t, J = 7.6 Hz), 7.42 (2H, t, J = 8.4 Hz), 7.52 (2H, d, J = 8.0 Hz), 8.19 (2H, d, J = 8.4 Hz). FAB-MS m/z: 247 $(M+H)^+$. HR-FAB-MS m/z: $(M+H)^+$ calcd for $C_{14}H_{12}ClO_2$, 247.0527; found, 247.0527.

5.2.17. Phenyl 4-(nitrooxymethyl)benzoate (13)

Compound **13** was synthesized using $AgNO_3$ (0.34 g, 2.03 mmol) and **12** (0.10 g, 0.41 mmol) in the conventional manner (colorless needles, 0.08 g, 0.29 mmol, 70.8%). Mp 108.3–109.2 °C. IR: 1735.8, 1618.2, 1280.6, 881.4, 752.2, 688.5 cm^{-1}. ^1H NMR: δ 5.52 (2H, s), 7.22 (1H, t, J = 8.2 Hz), 7.30 (2H, d, J = 8.0 Hz), 7.44 (2H, t, J = 8.0 Hz), 7.55 (2H, d, J = 8.0 Hz), 8.25 (2H, d, J = 6.4 Hz). FAB-MS m/z: 274 $(M+H)^+$. HR-FAB-MS m/z: $(M+H)^+$ calcd for $C_{14}H_{12}NO_5$, 274.0716; found, 274.0714.

5.3. Cells, animals, and antibodies

HCT116 and SW620 cells were cultured in McCoy's 5A medium. SW480, SKBr-3, MCF7 and MDA-MB-231 cells were cultured in RPMI1640 medium. CCD-1059SK cells were cultured in MEM. HT1080 cells were cultured in DMEM. All the culture media were supplemented with 10% fetal bovine serum (FBS), 50 μg/mL penicillin G, and 50 μg/mL streptomycin sulfate (Invitrogen) in an atmosphere of 5% CO_2 and 95% air at 37 °C. The mice were used at 6 weeks of age. Antibodies specific to anti-α-tubulin and β-actin were purchased from Sigma to Aldrich, and anti-phospho-histone H3 (Ser 10) was from Cell signaling.

5.4. Cell growth inhibition assay

Compounds were screened for cytotoxicity against seven mammalian cell lines representing different tissue types: cells were grown in the presence of the compounds for 72 h before growth was quantified using a Cell Counting Kit. The compounds were tested at final concentrations of 1, 10, 25, 50, 100, and 200 μM.

5.5. Examination of cell cycle regulation by flow cytometry

HCT116 cells were plated onto 60 mm diameter dishes (1.0×10^6/dish). After incubating for 24 h, the cells were washed with serum-free medium (2×1 mL) and immersed in serum-free medium (5 mL) for 24 h. After removal of the medium, the cells were washed with serum-free medium (2×1 mL) and incubated with **2a**, **8a** (each 20 μM), NCX4040 (40 μM), vincristine (150 nM), or control (0.4% DMSO) in the serum-free medium (5 mL) for another 24 h. The medium (about 5 mL) was transferred to Centrifuge Tubes (IWAKI). The adhered cells, after being washed twice with cold PBS (each 1 mL), were treated with trypsin 0.25% (1×) (Invitrogen) (200 μL) for 3 min and transferred to the above tubes. The cells in the tubes were treated with a Cycle Test Plus DNA reagent Kit (Cat. #340242) according to the procedure recommended by Becton Dickinson and Company. DNA content was measured with a FACS™Cant II.

5.6. Western blot analysis of phospho-histone H3 levels

HCT116 cells were plated onto 60 mm diameter dishes (1.0×10^6/dish). After incubating for 24 h, the cells were treated and incubated with **2a**, **8a**, NCX4040 (each 20 and 40 μM), vincristine (150 nM), or control (0.4% DMSO) in the same way as for the cell cycle test. The medium was discarded, and floating and adhered cells were washed with PBS (2×1 mL), scraped,, and resuspended in 400 μL of modified Covance Research lysis buffer (pH 8.0 and 1% Nonidet P-40 were adopted in place of pH 7.4 and 1% Triton-X 100, respectively) at 0 °C for 1 h. The lysates were centrifuged at 14000 ×*g* for 15 min at 4 °C. The protein concentration was determined with a BCA protein assay Kit (Thermo Fisher Scientific). An equal amount (7.5 μg) of protein was then resolved by SDS–PAGE and transferred to a PVDF membrane. The blots (1 × Tris–HCl buffer saline, 5% nonfat milk and 0.05% Tween 20 or 1 × Tris–HCl buffer saline, 12.5 mM NaF, 1% nonfat milk, 1% BSA, and 0.05% Tween 20) were probed with an antibody specific to each protein and were detected by using ECL chemiluminescence.

5.7. Flow cytometric analysis of phospho-histone H3 levels[21]

HCT116 cells were plated onto 60 mm diameter dishes (1.0×10^6/dish). After incubation for 24 h, the cells were treated and incubated with **2a**, **8a** (each 20 μM), NCX4040 (40 μM), vincristine (150 nM), or control (0.4% DMSO) in the same way as for the examination of cell cycle regulation. The cells were centrifuged at 190×*g* for 7 min, washed with PBS (2×5 mL), and fixed with PBS (1 mL) and 80% ice-cold ethanol (5 mL) for 2 h at −20 °C. The cells were centrifuged at 190×*g* for 7 min, washed twice with PBS (containing 1% BSA) (5 mL) and permeabilized by PBS (containing 1% BSA, 0.25% TritonX-100) (1 mL) for 5min at 0 °C. The cells were washed with PBS (5 mL), blocked with PBS (containing 1% BSA) (200 μl) for 2 h at room temperature, and incubated overnight at 4 °C with anti-body (phospho-histone H3 (1:100)). The cells were washed with PBS (containing 1% BSA)) (5 mL) twice, and incubated for 1 h at 4 °C with secondary anti-body (rabbit (1:40)). The cells were further washed with PBS (containing BSA) (1 mL), and incubated with propidium iodide (5 μg/ml in PBS) (500 μL) and RNase A (10 mg/ml) (25 μL) for 30 min at 37 °C. Dual label cell sorting was performed by FACS™Cant II.

5.8. TUNEL assay by flow cytometry

HCT116 cells were plated onto 60 mm diameter dishes (1.0×10^6/dish). After incubating for 24 h or 48 h, the cells were treated and incubated with **2a**, **8a** (each 20 μM), NCX4040 (40 μM), vincristine (150 nM), or control (0.4% DMSO) in the usual way. The floating and adhered cells were subjected to a TUNEL assay using the DeadEnd™ Fluorometirc TUNEL System according to the procedure (Cat. #G3250) by Promega.

5.9. Immunofluorescent staining of tubulin

The effects of the test compounds on microtubule structures were examined in HT1080 human fibrosarcoma cells as reported previously.[17]

5.10. Tubulin in vitro polymerization assay

Compounds **2a**, **8a** or vincristine was dissolved in General Tubulin Buffer containing 22% DMSO (220 μM for **2a** and **8a**; 110 μM for vincristine). For vehicle, General Tubulin Buffer containing 22% DMSO was used. An aliquot (5 μL) of each solution was transferred to a 96-well plate and allowed to warm at 37 °C. The tubulin solution was prepared by dissolving a purified tubulin (120 μL of 10 mg/mL General Tubulin Buffer) in the tubulin reaction mixture (368 μL of General Tubulin Buffer, 99.6 μL of Tubulin Glycerol Buffer, 6 μL of 100 mM GTP stock solution, and 6 μL of 1 mg/mL DAPI solution). An aliquot (50 μL) of this tubulin solution (2.0 mg/mL) was added to the solutions of **2a**, **8a** (20 μM), vincristine (10 μM) or control (2.0% DMSO) prewarmed in the 96-well plate at 37 °C. The polymerization was measured over 100 min by reading the increase in fluorescent emission at 460 nm in the kinetic mode with excitation at 340 nm.

5.11. In vivo antitumor activity

HCT116 cells (1.0×10^6/100 μL medium) were injected subcutaneously into the back of nude mice (6 weeks of age). Compound **8a** (1.0 mg or 1.6 mg/200 μL) and vehicle (10% castor oil in 1 × PBS, 200 μL) were intraperitoneally administered to the mice with 54.1–108.6 mm^3 ($n = 6$, respectively) at days 0, 2, 4, 7, 9, 11, 14, and 16, respectively. Tumor length and width as well as weights of mice were monitored for 21 days. Tumor volume (mm^3) was calculated by measuring length and width (in mm) as described.[22] *T*/*C* was calculated by dividing tumor volume for treated mice by tumor volume for control mice.

5.12. Statistical analysis

The statistical significance of the effects of drugs versus the control was analyzed with Student's *t*-test.

Acknowledgments

Part of this work was supported by the Strategic Project to Support the Formation of Research Bases at Private Universities. This is a product of research financially supported in part by Kansai University Research Grants: Grant-in-aid for Joint Research, 2009–2010.

References and notes

1. Rosetti, M.; Tesei, A.; Ulivi, P.; Fabbri, F.; Vannini, I.; Brigliadori, G.; Amadori, D.; Bolla, M.; Zoli, W. *Apoptosis* **2003**, *8*, 1321.
2. Nilima Shukla, N.; Angelini, G. D.; Ascione, R.; Talpahewa, S.; Capoun, R.; Jeremy, J. Y. *Ann. Thorac. Surg.* **2003**, *75*, 1437.
3. Tesei, A.; Ulivi, P.; Fabbri, F.; Rosetti, M.; Leonetti, C.; Scarsella, M.; Zupi, G.; Amadori, D.; Bolla, M.; Zoli, W. *J. Trans. Med.* **2005**, *3*, 7.
4. Fabbri, F.; Brigliadori, G.; Ulivi, P.; Tesei, A.; Vannini, I.; Rosetti, M.; Bravaccini, S.; Amadori, D.; Bolla, M.; Zoli, W. *Apoptosis* **2005**, *10*, 1095.
5. Bratasz, A.; Selvendiran, K.; Wasowicz, T.; Bobko, A.; Khramtsov, V.; Ignarro, L. J.; Kuppusamy, P. *J. Trans. Med.* **2008**, *6*, 9.
6. Tesei, A.; Zoli, W.; Fabbri, F.; Leonetti, C.; Rosetti, M.; Bolla, M.; Amadori, D.; Silvestrini, R. *Nitric Oxide* **2008**, *19*, 225.
7. Takeuchi, K.; Mizoguchi, H.; Araki, H.; Komoike, Y.; Suzuki, K. *Dig. Dis. Sci.* **2001**, *46*, 1805.
8. Huguenin, S.; Vacherot, F.; Fleury-Feith, J.; Riffaud, J. P.; Chopin, D. K.; Bolla, M.; Jaurand, M. C. *Cancer Lett.* **2005**, *218*, 163.
9. Rao, C. V.; Reddy, B. S.; Steele, V. E.; Wang, C.-X.; Liu, X.; Ouyang, N.; Patlolla, J. M. R.; Simi, B.; Kopelovich, L.; Rigas, B. *Mol. Cancer Ther.* **2006**, *5*, 1530.
10. Hulsman, N.; Medema, J. P.; Bos, C.; Jongejan, A.; Leurs, R.; Smit, M. J.; de Esch, I. J.; Richel, D.; Wijtmans, M. *J. Med. Chem.* **2007**, *50*, 2424.
11. Juan, G.; Traganos, F.; James, W. M.; Ray, J. M.; Roberge, M.; Sauve, D. M.; Anderson, H.; Darzynkiewicz, Z. *Cytometry* **1998**, *32*, 71.
12. Himes, R. H.; Kersey, R. N.; Heller-Bettinger, I.; Samson, F. E. *Cancer Res.* **1976**, *36*, 3798.
13. Hans, F.; Dimitrov, S. *Oncogene* **2001**, *20*, 3021.
14. Giet, R.; Glover, D. *J. Cell Biol.* **2001**, *152*, 669.
15. Adams, R. R.; Maiato, H.; Earnshaw, W. C.; Carmena, M. *J. Cell Biol.* **2001**, *153*, 865.
16. Wang, Y.; Zhang, W.; Jin, Y.; Johansen, J.; Johansen, K. M. *Cell* **2001**, *105*, 433.
17. Kohno, M.; Watanabe, K.; Tanimura, S. *Jpn. J. Cancer Chemother.* **2004**, *31*, 501.
18. Kumar, N. *J. Biol. Chem.* **1981**, *256*, 10435.
19. Bonne, D.; Heuséle, C.; Simon, C.; Pantaloni, D. *J. Biol. Chem.* **1985**, *260*, 2819.
20. Dojindo, http://www.dojindo.co.jp,2011.
21. Mi, L.; Xiao, Z.; Hood, B. L.; Dakshanamurthy, S.; Wang, X.; Govind, S.; Conrads, T. P.; Veenstra, T. D.; Chung, F. L. *J. Biol. Chem.* **2008**, *283*, 22136.
22. Komatsu, Y.; Tomizaki, K.; Tsukamoto, M.; Kato, T.; Nishino, N.; Sato, S.; Yamori, T.; Tsuruo, T.; Furumai, R.; Yoshida, M.; Horinouchi, S.; Hayashi, H. *Cancer Res.* **2001**, *61*, 4459.